Research Article

OUTAGE PERFORMANCE OF ENERGY HARVESTING ASSISTED MULTI-HOP M2M NETWORKS WITH PARTIAL RELAY SELECTION METHODS

Ngo Hoang AN[1,2], *Nguyen Trong HUAN*[3], *Ngoc-Lan NGUYEN*[3], *Nguyen Tien TUNG*[1,*]

[1]Faculty of Electronics Technology, Industrial University of Ho Chi Minh City (IUH), Ho Chi Minh City, Vietnam
[2]Ho Chi Minh City University of Industry and Trade (HUIT), Ho Chi Minh City, Vietnam
[3]Posts and Telecommunications Institute of Technology Ho Chi Minh city, Vietnam

annh@huit.edu.vn, huannt@ptithcm.edu.vn, lannn@ptit.edu.vn, nguyentientung@iuh.edu.vn

[*]Corresponding author: Nguyen Tien Tung; nguyentientung@iuh.edu.vn

DOI: 10.15598/aeee.v22i4.240407

Article history: Received Apr 18, 2024; Revised Jun 09, 2024; Accepted Jun 25, 2024; Published Dec 31, 2024.

Abstract. *This paper evaluates outage performance of wireless energy harvesting-assisted multi-hop mobile-to-mobile schemes. In our scheme, a mobile source sends its data to a mobile destination via a pre-established route, utilizing multiple intermediate mobile relays. The source and relay nodes harvest energy from a power beacon station deployed in the network, and they use this energy to transmit the data. To enhance reliability of data transmission, cooperative communication is employed at each hop, with assistance of outer mobile nodes (they are not on the source-to-destination route). An incremental cooperation technique is applied at each hop, i.e., cooperative communication is only performed when the direct link is outage. Moreover, two partial relay selection algorithms are also considered at each hop. This paper calculates end-to-end outage probability of the proposed schemes over double-Rayleigh fading channels. The obtained results show that our schemes can achieve better outage performance, as compared with the conventional multi-hop relay scheme and a corresponding scheme that uses random relay selection at each hop.*

Keywords

Mobile-to-mobile networks, multi-hop relaying, cooperative communication, partial relay selection, double-Rayleigh fading channel.

1. Introduction

Relaying methods [1], [2], [3], [4], [5], [6], [7] are currently being employed in various applications to enhance performance for next-generation wireless communication networks. For instance, dual-hop schemes utilizing full-duplex (FD) relays are proposed in [8], [9]. FD relaying offers a higher data rate/throughput, as compared with the corresponding half-duplex (HD) one. However, FD relays must engage in the challenging task of self-interference cancellation. The authors in [10], [11] investigate decode-and-forward (DF) relaying cognitive radio networks, where secondary users must adjust their transmit power to meet a required interference threshold. Due to the limitation of transmit power, the one-way and two-way relaying techniques [10], [11] are employed to improve outage probability (OP) performance for the secondary networks. The authors in [12], [13] study the OP performance of mobile-to-mobile (M2M) relaying networks. In the

M2M networks, devices are mobile nodes and channels between them are modeled as double-Rayleigh fading [12], [13]. In [14], [15], intelligent reflecting surfaces (IRS) are deployed to assist data transmission between a transmitter and a receiver, instead of using the relay nodes. Published works [16], [17], [18], [19], [20] consider multi-hop schemes, where the source data reaches the destination via multiple hops (or relays). In [16], a multi-hop secure communication scenario with presence of an active eavesdropper is examined. The authors in [17] design multi-hop schemes for short-packet communication networks. In [18], outage performance of multi-hop FD relaying models using non-orthogonal multiple access (NOMA) is evaluated. The authors in [19] investigate trade-off between security and reliability for multi-hop M2M networks operating on the cognitive environment, under impact of hardware noises. In [20], a hybrid relay/IRS based multi-hop network is designed.

In [21], [22], [23], [24], [25], [26], [27], wirelessly energy harvesting (WEH)-based multi-hop relay models are proposed and analyzed. In [21], [22], the secondary source and relay nodes harvest energy from power beacon stations deployed in the secondary networks. Then, they utilize this energy to transmit the source data to the secondary destination. In [23], the transmit power of the secondary transmitters depends on the maximal interference threshold given by the primary network, the channel gain between themselves and active eavesdroppers, and the energy harvested from the power beacon stations. To improve the outage performance for the secondary network, the authors in [23] propose various path-selection strategies. Unlike [23], published work [24] proposes a cooperative routing approach, where the secondary relay and destination nodes on the source-to-destination route attempt to receive the signals transmitted by their previous nodes. This approach significantly enhances the decoding possibility of the secondary nodes. In [25], the secondary source is equipped with multiple antennas, and an efficient relay selection method at each hop is proposed. In particular, the secondary nodes in [25] are grouped in clusters, and at each hop, one of the cluster nodes is selected for receiving and then forwarding the source data to the next hop. The results obtained present that the path-selection methods in [23], the cooperative routing method in [24] and the hop-by-hop relay selection method in [25] achieve much better performance, as compared with the conventional multi-hop relaying schemes in [21], [22]. However, implementing the schemes in [23], [24], [25] is very complex because they require high synchronization between the nodes. In [26], the authors propose a simple WEH-based multi-hop relay scheme using cooperative communication at each hop. In cooperative communication [26], [28], both direct link and relay link are exploited to enhance the decoding possibility at the receivers.

In this paper, we study WEH-based multi-hop M2M schemes using hop-by-hop cooperative transmission. Unlike [21], [22], [23], [24], [25], [26], this paper focuses on M2M communication networks, where all nodes are mobile. Different with [29], we consider multi-hop M2M scheme with two partial relay selection (PRS) methods employed at each hop. In [19], the authors evaluate the end-to-end OP (OP-e2e) and end-to-end intercept probability of multi-hop M2M schemes in the cognitive radio environment. In contrast to [19], this paper employs cooperative communication at each hop to enhance the performance. To the best of our knowledge, our previous work [30] is most relevant to this paper. However, [30] only considers the cooperative communication with a single relay at each hop, while our work explores a multi-relay scheme using relay selection methods.

The following summarizes the new points and main contributions of our work:

- Firstly, the incremental cooperation method [26], and PRS method [26] are applied since they are simple to implement. Moreover, we consider two PRS methods, where the best relay can be selected by using channel state information (CSI) of either the first link or the second link. It is noteworthy that the PRS method in [26] only utilizes CSI of the first link for the relay selection process.
- Secondly, we evaluate the performance of the proposed schemes over double-Rayleigh fading channels through both theoretical analysis and simulations.
- Thirdly, the results present that our schemes can achieve better performance, as compared with the conventional multi-hop scheme [19] and the corresponding one using random relay selection [30].
- Finally, impact of the important parameters (i.e., transmit power of the power beacon station, number of hops, fraction of time spent for the EH phase) on the performance is investigated.

The remaining contents of this paper are summarized as follows: Section 2. presents the system model of the proposed schemes. Derivation of OP is carried out in Section 3. . Simulation and theoretical results are provided in Section 4. , and Section 5. concludes this paper.

2. System Model

Fig. 1 illustrates the system model of the multi-hop M2M scheme, where the source (M_1) sends its data to the destination (M_{K+1}) through an K-hop route

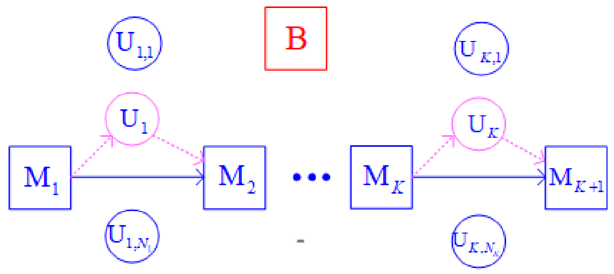

Fig. 1: Multi-hop M2M scheme using cooperative communication.

pre-established at the network layer. The route establishment is performed at the network layer, and it is assumed that the route is available before the data transmission starts. Nodes on the $\mathrm{M}_1 \to \mathrm{M}_K$ route are respectively denoted by M_2, M_3, ..., M_K, where M_p is the pth nearest to the source M_1 with $p = 2, 3, ..., K$. At the kth hop, there are N_k $(N_k \geq 1)$ nodes that are available to assist the data transmission between M_k and M_{k+1}, where $k = 1, 2, ..., K$. These nodes are denoted as $\mathrm{U}_{k,1}$, $\mathrm{U}_{k,2}$,..., U_{k,N_k}. Additionally, only one of these nodes is selected to help the $\mathrm{M}_k \to \mathrm{M}_{k+1}$ transmission. For ease of presentation, we denote the selected node as U_k, where $\mathrm{U}_k \in \{\mathrm{U}_{k,1}, \mathrm{U}_{k,2}, ..., \mathrm{U}_{k,N_k}\}$. To transmit the data, the M_k and U_k nodes will harvest energy from the power station (denoted by B). All the nodes are assumed to be mobile, and are equipped with a single antenna. It is also assumed that the M_k and U_k nodes use the DF technique to relay the source data from M_1 to M_{K+1}.

Let us denote g_{XY} and d_{XY} as channel gain and distance of the X $\to$ Y link, respectively, where X,Y $\in \{\mathrm{M}_k, \mathrm{U}_{k,t}, \mathrm{B}\}$, $k = 1, 2, ..., K+1$, $t = 1, 2, ..., N_k$. Assume that the nodes $\mathrm{U}_{k,t}$ are close together, i.e., they are in a cluster [31], and we assume that $d_{\mathrm{XU}_{k,t}} = d_{\mathrm{XU}_k}$ and $d_{\mathrm{U}_{k,t}\mathrm{Y}} = d_{\mathrm{U}_k\mathrm{Y}}$, for all X, Y, k and t. We also denote P_{X} and σ_0^2 as transmit power of the node X and variance of Gaussian noise at all the receivers, respectively.

If the delay of the $\mathrm{M}_1 \to \mathrm{M}_K$ transmission is $L = 1$, and time allocated for the $k$thhop is $\chi = L/K = 1/K$, $\forall k$. Considering the kth hop; there are three phases as (see [30]): i) the first phase (the EH phase) whose time is $\alpha\chi$ is used by M_k and U_k for harvesting energy from B; ii) the second phase whose time is $(1-\alpha)\chi/2$ is used to transmit the source data from M_k to U_k and M_{k+1}; iii) the third phase whose time is $(1-\alpha)\chi/2$ is used to relay the source data from U_k to M_{k+1} (if required).

Remark 1. *We first note that $\alpha\,(0 < \alpha < 1)$is a pre-designed parameter. As shown in [30], the value of α needs to be designed appropriately to achieve the best system performance. Next, with the incremental cooperation technique used, if the $M_k \to M_{k+1}$ transmission is successful, U_k is not required to retransmit the received data to M_{k+1} [30].*

Similar to [30], the energy harvested by M_k and U_k during the EH phase can be expressed as

$$\begin{aligned} \mathrm{EH}_{\mathrm{M}_k} &= \eta\alpha\chi P_{\mathrm{B}} d_{\mathrm{BM}_k}^{-\beta} g_{\mathrm{BM}_k}, \\ \mathrm{EH}_{\mathrm{U}_k} &= \eta\alpha\chi P_{\mathrm{B}} d_{\mathrm{BU}_k}^{-\beta} g_{\mathrm{BU}_k}, \end{aligned} \quad (1)$$

where $\beta\,(2 \leq \beta \leq 6)$ is a path-loss factor and η is a conversion efficiency.

From (1), we can formulate transmit power of M_k and U_k, respectively as

$$\begin{aligned} P_{\mathrm{M}_k} &= \frac{\mathrm{EH}_{\mathrm{M}_k}}{(1-\alpha)\,\chi/2} = \mu\lambda_{\mathrm{BM}_k} P_{\mathrm{B}} g_{\mathrm{BM}_k}, \\ P_{\mathrm{U}_k} &= \frac{\mathrm{EH}_{\mathrm{U}_k}}{(1-\alpha)\,\chi/2} = \mu\lambda_{\mathrm{BU}_k} P_{\mathrm{B}} g_{\mathrm{BU}_k}, \end{aligned} \quad (2)$$

where $\mu = 2\eta\alpha/(1-\alpha)$, $\lambda_{\mathrm{BM}_k} = d_{\mathrm{BM}_k}^{-\beta}$ and $\lambda_{\mathrm{BU}_k} = d_{\mathrm{BU}_k}^{-\beta}$.

Using (2), we can formulate the instantaneous channel capacity of the $\mathrm{M}_k \to \mathrm{M}_{k+1}$ link as

$$\begin{aligned} C_{\mathrm{M}_k\mathrm{M}_{k+1}} &= \frac{(1-\alpha)\,\chi}{2}\log_2\left(1 + \frac{P_{\mathrm{M}_k} d_{\mathrm{M}_k\mathrm{M}_{k+1}}^{-\beta} g_{\mathrm{M}_k\mathrm{M}_{k+1}}}{\sigma_0^2}\right) \\ &= \frac{(1-\alpha)\,\chi}{2}\log_2\left(1 + \mu\lambda_{\mathrm{BM}_k}\lambda_{\mathrm{M}_k\mathrm{M}_{k+1}}\Delta g_{\mathrm{BM}_k} g_{\mathrm{M}_k\mathrm{M}_{k+1}}\right), \end{aligned} \quad (3)$$

where $\lambda_{\mathrm{M}_k\mathrm{M}_{k+1}} = d_{\mathrm{M}_k\mathrm{M}_{k+1}}^{-\beta}$ and $\Delta = P_{\mathrm{B}}/\sigma_0^2$.

Similarly, the instantaneous channel capacity of the $\mathrm{M}_k \to \mathrm{U}_k$ and $\mathrm{U}_k \to \mathrm{M}_{k+1}$ links can be expressed, respectively as

$$\begin{aligned} C_{\mathrm{M}_k\mathrm{U}_k} &= \frac{(1-\alpha)\,\chi}{2} \\ &\times \log_2\left(1 + \mu\lambda_{\mathrm{BM}_k}\lambda_{\mathrm{M}_k\mathrm{U}_k}\Delta g_{\mathrm{BM}_k} g_{\mathrm{M}_k\mathrm{U}_k}\right), \\ C_{\mathrm{U}_k\mathrm{M}_{k+1}} &= \frac{(1-\alpha)\,\chi}{2} \\ &\times \log_2\left(1 + \mu\lambda_{\mathrm{BU}_k}\lambda_{\mathrm{U}_k\mathrm{M}_{k+1}}\Delta g_{\mathrm{BU}_k} g_{\mathrm{U}_k\mathrm{M}_{k+1}}\right), \end{aligned} \quad (4)$$

where $\lambda_{\mathrm{M}_k\mathrm{U}_k} = d_{\mathrm{M}_k\mathrm{U}_k}^{-\beta}$ and $\lambda_{\mathrm{U}_k\mathrm{M}_{k+1}} = d_{\mathrm{U}_k\mathrm{M}_{k+1}}^{-\beta}$.

Now, we present two considered PRS methods. In the first PRS method, named C-PRS (Conventional PRS), the best relay U_k is selected as in [26]:

$$\text{C-PRS: } g_{\mathrm{M}_k\mathrm{U}_k} = \max_{t=1,2,\ldots,N_k}\left(g_{\mathrm{M}_k\mathrm{U}_{k,t}}\right). \quad (5)$$

In the second PRS method, named M-PRS (Modified PRS), the best relay U_k is chosen as

$$\begin{aligned} \mathrm{M-PRS}: P_{\mathrm{U}_k} g_{\mathrm{U}_k\mathrm{M}_{k+1}} &= \max_{t=1,2,\ldots,N_k}\left(P_{\mathrm{U}_{k,t}} g_{\mathrm{U}_{k,t}\mathrm{M}_{k+1}}\right) \\ \Leftrightarrow g_{\mathrm{BU}_k} g_{\mathrm{U}_k\mathrm{M}_{k+1}} &= \max_{t=1,2,\ldots,N_k}\left(g_{\mathrm{BU}_{k,t}} g_{\mathrm{U}_{k,t}\mathrm{M}_{k+1}}\right). \end{aligned} \quad (6)$$

Remark 2. *The main idea of the C-PRSand M-PRSmethods is that the best relay is selected to maximize the instantaneous signal-to-noise ratio (SNR) of either the first relaying link (the $M_k \to U_{k,t}$ links) or the second relaying link (the $U_{k,t} \to M_{k+1}$ links). It is noted that because M_k and $U_{k,t}$ are within radio range of each other, we can assume that M_k can know CSI of all the $M_k \to U_{k,t}$ links. Therefore, M_k in the C-PRS scheme can select the cooperative relay by using (5). Similarly, M_{k+1} in the M-PRS scheme can obtain CSI of all the $U_{k,t} \to M_k$ links. However, to perform the relay selection algorithm in (6), all the nodes $U_{k,t}$ have to estimate $g_{BU_{k,t}}$, and then send this value to M_{k+1}. Hence, we observe that the M-PRS scheme is more complex to implement, as compared to C-PRS. It is due to the fact that the implementation of M-PRS requires CSI of the $B \to U_{k,t}$ and $U_{k,t} \to M_{k+1}$ links.*

Next, probability that the data transmission at the kth hop in the proposed Z scheme is outage can be formulated as

$$\begin{aligned}
\mathrm{OP}_k^{\mathrm{Z}} &= \underbrace{\Pr\left(C^{\mathrm{Z}}_{\mathrm{M}_k\mathrm{M}_{k+1}} < R_{\mathrm{th}}, C^{\mathrm{Z}}_{\mathrm{M}_k\mathrm{U}_k} < R_{\mathrm{th}}\right)}_{\mathrm{OP}_{k,1}} + \\
&\Pr\left(C^{\mathrm{Z}}_{\mathrm{M}_k\mathrm{U}_k} \geq R_{\mathrm{th}}, C^{\mathrm{Z}}_{\mathrm{M}_k\mathrm{M}_{k+1}} < R_{\mathrm{th}}, C^{\mathrm{Z}}_{\mathrm{U}_k\mathrm{M}_{k+1}} < R_{\mathrm{th}}\right) \\
&= \mathrm{OP}^{Z}_{k,1} + \underbrace{\Pr\left(C^{\mathrm{Z}}_{\mathrm{M}_k\mathrm{U}_k} \geq R_{\mathrm{th}}, C^{\mathrm{CC}}_{\mathrm{M}_k\mathrm{M}_{k+1}} < R_{\mathrm{th}}\right)}_{\mathrm{OP}^{Z}_{k,2}} \\
&\times \underbrace{\Pr\left(C^{\mathrm{Z}}_{\mathrm{U}_k\mathrm{M}_{k+1}} < R_{\mathrm{th}}\right)}_{\mathrm{OP}^{Z}_{k,3}} \\
&= \mathrm{OP}^{Z}_{k,1} + \mathrm{OP}^{Z}_{k,2} \times \mathrm{OP}^{Z}_{k,3},
\end{aligned} \tag{7}$$

where Z $\in$ {C-PRS,M-PRS} and R_{th} is a predetermined outage threshold.

In (7), $\mathrm{OP}^{Z}_{k,1}$ is probability that the $\mathrm{M}_k \to \mathrm{U}_k$ and $\mathrm{M}_k \to \mathrm{M}_{k+1}$ links are outage. Next, $\mathrm{OP}^{Z}_{k,2}$ is probability that M_{k+1} cannot decode the data received from M_k successfully, and U_k successfully decodes it. Finally, $\mathrm{OP}^{Z}_{k,3}$ is probability that the $\mathrm{U}_k \to \mathrm{M}_{k+1}$ transmission fails. Due to the DF relaying technique used, OP-e2e of the proposed Z scheme can be expressed as

$$\mathrm{OP}^{\mathrm{Z}}_{\mathrm{e2e}} = 1 - \prod_{k=1}^{K}\left(1 - \mathrm{OP}^{\mathrm{Z}}_k\right), \tag{8}$$

where $1-\mathrm{OP}^{\mathrm{Z}}_k$ is probability that the data transmission at the kth hop is successful.

3. Performance Analysis

This section derives OP-e2e of C-PRSand M-PRS. Firstly, we find $\mathrm{OP}_k^{\text{C-PRS}}$ and $\mathrm{OP}_k^{\text{M-PRS}}$, and then substitute them into (8) to obtain $\mathrm{OP}_{\mathrm{e2e}}^{\text{C-PRS}}$ and $\mathrm{OP}_{\mathrm{e2e}}^{\text{M-PRS}}$.

3.1. Double-Rayleigh fading channel

Since the nodes X and Y are mobile, X,Y $\in \{\mathrm{M}_k, \mathrm{U}_{k,t}, \mathrm{B}\}$, the X-Y link experiences double-Rayleigh fading channel. As in [30], cumulative distribution function (CDF) and probability density function (PDF) of g_{XY} is written, respectively as

$$\begin{aligned}
F_{g_{\mathrm{XY}}}(x) &= 1 - 2\sqrt{x}K_1\left(2\sqrt{x}\right), \\
f_{g_{\mathrm{XY}}}(x) &= 2K_0\left(2\sqrt{x}\right),
\end{aligned} \tag{9}$$

where $K_i(.)\,(i=0,1)$ is the ith order modified Bessel function of the second kind [32].

Combining (5) and (9), CDF of $g_{\mathrm{M}_k\mathrm{U}_k}$ is given as

$$\begin{aligned}
F_{g_{\mathrm{M}_k\mathrm{U}_k}}(x) &= \Pr\left(\max_{t=1,2,\ldots,N_k}\left(g_{\mathrm{M}_k\mathrm{U}_{k,t}}\right) < x\right) \\
&= \prod_{t=1}^{N_k}\Pr\left(g_{\mathrm{M}_k\mathrm{U}_{k,t}} < x\right) = \prod_{t=1}^{N_k} F_{g_{\mathrm{M}_k\mathrm{U}_{k,t}}}(x) \\
&= \left[1 - 2\sqrt{x}K_1\left(2\sqrt{x}\right)\right]^{N_k}.
\end{aligned} \tag{10}$$

Next, setting $W_t = g_{\mathrm{BU}_{k,t}} g_{\mathrm{U}_{k,t}\mathrm{M}_{k+1}}$; CDF of W_t can be formulated as

$$\begin{aligned}
F_{W_t}(x) &= \Pr\left(g_{\mathrm{BU}_{k,t}} g_{\mathrm{U}_{k,t}\mathrm{M}_{k+1}} < x\right) \\
&= \int_0^{+\infty} F_{g_{\mathrm{BU}_{k,t}}}\left(\frac{x}{y}\right) f_{g_{\mathrm{U}_{k,t}\mathrm{M}_{k+1}}}(y)\, dy.
\end{aligned} \tag{11}$$

Substituting (9) into (11), we obtain a closed-form expression of $F_{W_t}(x)$ as

$$\begin{aligned}
F_{W_t}(x) &= \int_0^{+\infty}\left[1 - 2\sqrt{\frac{x}{y}}K_1\left(2\sqrt{\frac{x}{y}}\right)\right] 2K_0\left(2\sqrt{y}\right) dy \\
&= 1 - \int_0^{+\infty} 4\sqrt{\frac{x}{y}}K_0\left(2\sqrt{y}\right)K_1\left(2\sqrt{\frac{x}{y}}\right) dy \\
&= 1 - G^{4,0}_{0,4}\left(x \,\middle|\, \begin{matrix} - \\ 0,\ 1,\ 1,\ 1 \end{matrix}\right),
\end{aligned} \tag{12}$$

where $G^{:,:}_{:,:}(.|.)$ denotes MeijerG function [32].

Next, setting $W_{\max} = g_{\mathrm{BU}_k} g_{\mathrm{U}_k\mathrm{M}_{k+1}}$, from (6) and (12), we can write CDF of $W_{\max}$ as

$$\begin{aligned}
F_{W_{\max}}(x) &= \Pr\left(\max_{t=1,2,\ldots,N_k}\left(W_t\right) < x\right) \\
&= \prod_{t=1}^{N_k} F_{W_t}(x) = \left[1 - G^{4,0}_{0,4}\left(x \,\middle|\, \begin{matrix} - \\ 0,\ 1,\ 1,\ 1 \end{matrix}\right)\right]^{N_k}.
\end{aligned} \tag{13}$$

3.2. OP-e2e of C-PRS and M-PRS

We first rewrite $\mathrm{OP}_{k,1}^{\mathrm{Z}}$ in (7) under the following form:

$$\begin{aligned}\mathrm{OP}_{k,1}^{\mathrm{Z}} &= \Pr\left(g_{\mathrm{BM}_k} g_{\mathrm{M}_k\mathrm{M}_{k+1}} < \rho_{k,1}, g_{\mathrm{BM}_k} g_{\mathrm{M}_k\mathrm{U}_k} < \rho_{k,2}\right)\\ &= \Pr\left(g_{\mathrm{M}_k\mathrm{M}_{k+1}} < \frac{\rho_{k,1}}{g_{\mathrm{BM}_k}}, g_{\mathrm{M}_k\mathrm{U}_k} < \frac{\rho_{k,2}}{g_{\mathrm{BM}_k}}\right)\\ &= \int_0^{+\infty} F_{g_{\mathrm{M}_k\mathrm{M}_{k+1}}}\left(\frac{\rho_{k,1}}{x}\right) F_{g_{\mathrm{M}_k\mathrm{U}_k}}\left(\frac{\rho_{k,2}}{x}\right) f_{g_{\mathrm{BM}_k}}(x)\, dx,\end{aligned} \tag{14}$$

where $Z \in \{\text{C-PRS,M-PRS}\}$, and

$$\rho_{k,1} = \frac{2^{\frac{2R_{\mathrm{th}}}{(1-\alpha)\chi}} - 1}{\mu \lambda_{\mathrm{BM}_k} \lambda_{\mathrm{M}_k\mathrm{M}_{k+1}} \Delta}, \rho_{k,2} = \frac{2^{\frac{2R_{\mathrm{th}}}{(1-\alpha)\chi}} - 1}{\mu \lambda_{\mathrm{BM}_k} \lambda_{\mathrm{M}_k\mathrm{U}_k} \Delta}.$$

Combining (9)-(14), exact expressions of $\mathrm{OP}_{k,1}^{\text{C-PRS}}$ and $\mathrm{OP}_{k,1}^{\text{M-PRS}}$ can be given, respectively as

$$\begin{aligned}\mathrm{OP}_{k,1}^{\text{C-PRS}} = \int_0^{+\infty} \Bigg\{ &\left[1 - 2\sqrt{\frac{\rho_{k,1}}{x}} K_1\left(2\sqrt{\frac{\rho_{k,1}}{x}}\right)\right]\\ \times &\left[1 - 2\sqrt{\frac{\rho_{k,2}}{x}} K_1\left(2\sqrt{\frac{\rho_{k,2}}{x}}\right)\right]^{N_k} 2K_0\left(2\sqrt{x}\right)\Bigg\} dx,\end{aligned} \tag{15}$$

$$\begin{aligned}\mathrm{OP}_{k,1}^{\text{M-PRS}} = \int_0^{+\infty} \Bigg\{ &\left[1 - 2\sqrt{\frac{\rho_{k,1}}{x}} K_1\left(2\sqrt{\frac{\rho_{k,1}}{x}}\right)\right]\\ \times &\left[1 - 2\sqrt{\frac{\rho_{k,2}}{x}} K_1\left(2\sqrt{\frac{\rho_{k,2}}{x}}\right)\right] 2K_0\left(2\sqrt{x}\right)\Bigg\} dx.\end{aligned} \tag{16}$$

Next, $\mathrm{OP}_{k,2}^{\mathrm{Z}}$ in (7) can be formulated as

$$\begin{aligned}\mathrm{OP}_{k,2}^{\mathrm{Z}} &= \Pr\left(g_{\mathrm{BM}_k} g_{\mathrm{M}_k\mathrm{M}_{k+1}} < \rho_{k,1}, g_{\mathrm{BM}_k} g_{\mathrm{M}_k\mathrm{U}_k} \geq \rho_{k,2}\right)\\ &= \Pr\left(g_{\mathrm{M}_k\mathrm{M}_{k+1}} < \frac{\rho_{k,1}}{g_{\mathrm{BM}_k}}, g_{\mathrm{M}_k\mathrm{U}_k} \geq \frac{\rho_{k,2}}{g_{\mathrm{BM}_k}}\right)\\ &= \int_0^{+\infty} F_{g_{\mathrm{M}_k\mathrm{M}_{k+1}}}\left(\frac{\rho_{k,1}}{x}\right)\left[1 - F_{g_{\mathrm{M}_k\mathrm{U}_k}}\left(\frac{\rho_{k,2}}{x}\right)\right]\\ &\quad \times f_{g_{\mathrm{BM}_k}}(x)\, dx,\end{aligned} \tag{17}$$

where $Z \in \{\text{C-PRS,M-PRS}\}$.

Then, substituting (9)-(13) into (17), we can obtain exact expressions of $\mathrm{OP}_{k,2}^{\text{C-PRS}}$ and $\mathrm{OP}_{k,2}^{\text{M-PRS}}$, respectively as

$$\begin{aligned}\mathrm{OP}_{k,2}^{\text{C-PRS}} = \int_0^{+\infty} \Bigg\{ &\left[1 - 2\sqrt{\frac{\rho_{k,1}}{x}} K_1\left(2\sqrt{\frac{\rho_{k,1}}{x}}\right)\right] \times\\ &\left[1 - \left(1 - 2\sqrt{\frac{\rho_{k,2}}{x}} K_1\left(2\sqrt{\frac{\rho_{k,2}}{x}}\right)\right)^{N_k}\right] 2K_0\left(2\sqrt{x}\right)\Bigg\} dx,\end{aligned} \tag{18}$$

$$\begin{aligned}\mathrm{OP}_{k,2}^{\text{M-PRS}} = \int_0^{+\infty} \Bigg\{ &\left[1 - 2\sqrt{\frac{\rho_{k,1}}{x}} K_1\left(2\sqrt{\frac{\rho_{k,1}}{x}}\right)\right]\\ \times 4&\sqrt{\frac{\rho_{k,2}}{x}} K_1\left(2\sqrt{\frac{\rho_{k,2}}{x}}\right) K_0\left(2\sqrt{x}\right)\Bigg\} dx.\end{aligned} \tag{19}$$

For the probability $\mathrm{OP}_{k,3}^{\text{C-PRS}}$ in (7), using (12), we obtain the following result:

$$\begin{aligned}\mathrm{OP}_{k,3}^{\text{C-PRS}} &= \Pr\left(g_{\mathrm{BU}_k} g_{\mathrm{U}_k\mathrm{M}_{k+1}} < \rho_{k,3}\right)\\ &= 1 - G_{0,4}^{4,0}\left(\rho_{k,3}\middle|\begin{matrix}-\\0,\ 1,\ 1,\ 1\end{matrix}\right),\end{aligned} \tag{20}$$

where

$$\rho_{k,3} = \frac{2^{\frac{2R_{\mathrm{th}}}{(1-\alpha)\chi}} - 1}{\mu \lambda_{\mathrm{BU}_k} \lambda_{\mathrm{U}_k\mathrm{M}_{k+1}} \Delta}.$$

Finally, using (13), $\mathrm{OP}_{k,3}^{\text{M-PRS}}$ can be expressed by an exact closed-form expression as

$$\begin{aligned}\mathrm{OP}_{k,3}^{\text{M-PRS}} &= \Pr\left(\max_{t=1,2,\ldots,N_k}\left(g_{\mathrm{BU}_{k,t}} g_{\mathrm{U}_{k,t}\mathrm{M}_{k+1}}\right) < \rho_{k,3}\right)\\ &= \left[1 - G_{0,4}^{4,0}\left(\rho_{k,3}\middle|\begin{matrix}-\\0,\ 1,\ 1,\ 1\end{matrix}\right)\right]^{N_k}.\end{aligned} \tag{21}$$

3.3. OP-e2e of RRS and WoCC

This paper compares OP-e2e of the proposed C-PRS and M-PRS schemes with two corresponding schemes. In the first one, named RRS (Random Relay Selection), the random relay selection method is employed at each hop. This means that the U_k relay is randomly selected at the kth hop. In the second one, named WoCC (Without Cooperative Communication), direct transmission between M_k and M_{k+1} is performed at the kth hop, without using cooperative communication.

It is worth noting that the OP-e2e performance of the RRSscheme is same with that of the single-relay scheme proposed in [30]. Therefore, using the results obtained in [30], we can write OP at the kth hop in this scheme as

$$\mathrm{OP}_k^{\mathrm{RRS}} = \mathrm{OP}_{k,1}^{\mathrm{RRS}} + \mathrm{OP}_{k,2}^{\mathrm{RRS}} \times \mathrm{OP}_{k,3}^{\mathrm{RRS}}, \tag{22}$$

where

$$\begin{aligned}\mathrm{OP}_{k,1}^{\mathrm{RRS}} = \int_0^{+\infty} \Bigg\{ &\left[1 - 2\sqrt{\frac{\rho_{k,1}}{x}} K_1\left(2\sqrt{\frac{\rho_{k,1}}{x}}\right)\right] \times\\ &\left[1 - 2\sqrt{\frac{\rho_{k,2}}{x}} K_1\left(2\sqrt{\frac{\rho_{k,2}}{x}}\right)\right] 2K_0\left(2\sqrt{x}\right)\Bigg\} dx.\end{aligned} \tag{23}$$

$$\begin{aligned}\mathrm{OP}_{k,2}^{\mathrm{RRS}} = \int_0^{+\infty} \Bigg\{ &\left[1 - 2\sqrt{\frac{\rho_{k,1}}{x}} K_1\left(2\sqrt{\frac{\rho_{k,1}}{x}}\right)\right]\\ \times 4&\sqrt{\frac{\rho_{k,2}}{x}} K_1\left(2\sqrt{\frac{\rho_{k,2}}{x}}\right) K_0\left(2\sqrt{x}\right)\Bigg\} dx.\end{aligned} \tag{24}$$

$$\mathrm{OP}_{k,3}^{\mathrm{RRS}} = 1 - G_{0,4}^{4,0}\left(\rho_{k,3}\middle|\begin{matrix}-\\0,\ 1,\ 1,\ 1\end{matrix}\right). \tag{25}$$

Then, OP-e2eof RRS can be expressed as

$$\mathrm{OP}_{\mathrm{e2e}}^{\mathrm{RRS}} = 1 - \prod_{k=1}^{K}\left(1 - \mathrm{OP}_k^{\mathrm{RRS}}\right). \tag{26}$$

In the WoCC scheme, the direct transmission between the nodes M_k and M_{k+1} at the kth hop is used, for all $k = 1, 2, ..., K$. Indeed, at the kth hop, there are two phases: i) the first phase $(\alpha\chi)$ is used by M_k for harvesting the wirelessly energy from B; ii) the second phase $((1-\alpha)\chi)$ is used for the $M_k \to M_{k+1}$ data transmission. As a result, we can formulate the instantaneous channel capacity of the $M_k \to M_{k+1}$ link in this scheme as

$$C^{\rm WoCC}_{\rm M_k M_{k+1}} = (1-\alpha)\chi \times \log_2\left(1 + \frac{\eta\alpha}{1-\alpha}\lambda_{{\rm BM}_k}\lambda_{{\rm M}_k{\rm M}_{k+1}}\Delta g_{{\rm BM}_k} g_{{\rm M}_k{\rm M}_{k+1}}\right). \quad (27)$$

Then, OP at the kth hop can be exactly computed as

$$\begin{aligned} {\rm OP}^{\rm WoCC}_k &= \Pr\left(C^{\rm WoCC}_{\rm M_k M_{k+1}} < R_{\rm th}\right) \\ &= \Pr\left(g_{{\rm BM}_k} g_{{\rm M}_k{\rm M}_{k+1}} < \rho_{k,4}\right) \\ &= 1 - G^{4,0}_{0,4}\left(\rho_{k,4}\middle|\begin{matrix} - \\ 0,\ 1,\ 1,\ 1\end{matrix}\right), \end{aligned} \quad (28)$$

where

$$\rho_{k,4} = \frac{1-\alpha}{\eta\alpha\lambda_{{\rm BM}_k}\lambda_{{\rm M}_k{\rm M}_{k+1}}\Delta}\left(2^{\frac{R_{\rm th}}{(1-\alpha)\chi}} - 1\right). \quad (29)$$

From (28), OP-e2e of WoCC can be given by an exact closed-form expression as

$$\begin{aligned} {\rm OP}^{\rm WoCC}_{\rm e2e} &= 1 - \prod_{k=1}^{K}\left(1 - {\rm OP}^{\rm WoCC}_k\right) \\ &= 1 - \prod_{k=1}^{K} G^{4,0}_{0,4}\left(\rho_{k,4}\middle|\begin{matrix} - \\ 0,\ 1,\ 1,\ 1\end{matrix}\right). \end{aligned} \quad (30)$$

4. Simulation Results

In Section 4, we perform simulations to compare the OP-e2eperformance of the C-PRS, M-PRS, RRS and WoCC schemes as well as to verify the correctness of the given expressions. The simulation and theoretical results are denoted by 'Sim' and 'Theory', respectively. Indeed, all the figures below present that the 'Sim' and 'Theory' results are in a good agreement.

In all the simulations, the mobile node (M_k) is positioned at $((k-1)/K, 0)$, where $k = 1, 2, ..., K+1$. With this setup, all the nodes (M_k) are aligned on a straight line, the distance between the source (M_0) and the destination (M_{K+1}) is fixed by 1, and the distance between M_k and M_{k+1} is $d_{{\rm M}_k{\rm M}_{k+1}} = 1/K$, $\forall k$. For the outer relay U_k, this node is located at the middle of M_k and M_{k+1}, with position $((2k-1)/(2K), 0)$, $d_{{\rm M}_k M_{k+1}} = 1/K$, $\forall k$. Finally, position of the power beacon (B) is fixed at $(0.5, 0.5)$.

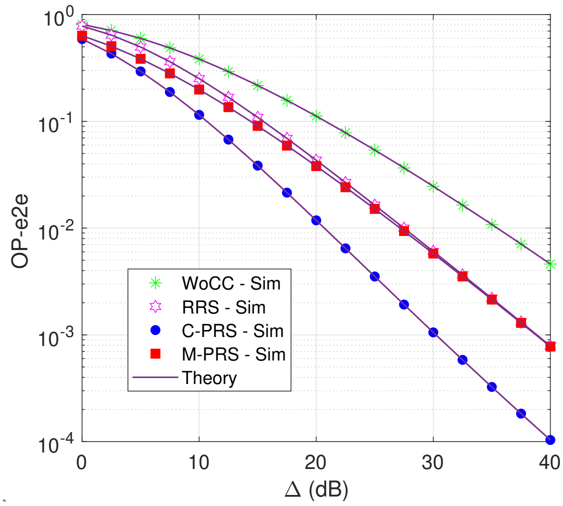

Fig. 2: OP-e2e as a function of Δ (dB) when $K = 4$, $N = 5$, $R_{\rm th} = 0.5$ and $\alpha = 0.35$.

To focus on analyzing impact of important system parameters on the OP-e2e performance of the considered schemes, we fix: $\beta = 3$ and $\eta = 1$. It is also assumed that the number of available relays at each hop is the same, i.e., $N_k = N$ $(\forall n)$. In Fig. 2, we present the OP-e2e performance of the C-PRS, M-PRS, RRS and WoCC schemes as a function of Δ in dB when $K = 4$, $N = 5$, $R_{\rm th} = 0.5$ and $\alpha = 0.35$. We first observe that all the schemes obtain better performance as increasing Δ. It is because increasing Δ also entails increasing the transmit power of the transmitters. Next, Fig. 2 shows that the schemes using cooperative communication obtain better performance as compared with WoCC. It is due to the fact that cooperative communication enhances reliability of the data transmission at each hop, as compared with the direct transmission. In addition, C-PRS and M-PRS outperform RRS due to usage of the PRS method. In this figure, C-PRS obtains the best performance, while performance ofM-PRSis only slightly better than that of RRS.

Fig. 3 investigates impact the number of relays at each hop (N) on the performance of the considered schemes when $\Delta = 20$ (dB), $K = 5$, $R_{\rm th} = 0.25$ and $\alpha = 0.25$. We again see that OP-e2e of C-PRS and WoCC is lowest and highest, respectively, and OP-e2e of M-PRS is slightly lower than that of RRS. It is also seen that OP-e2e of C-PRS significantly decreases with the increasing of N, but that of M-PRS slightly decreases. It is worth noting that the main disadvantage of M-PRS is that it only enhances the quality of channels at the second link. Consequently, its performance primarily relies on the quality of the first link. This is why performance of M-PRS slightly improves compared to RRS and remains relatively stable even with an increase in the number of relays at each hop. Finally, from Figs. 2 - 3, we can see that C-PRS achieves

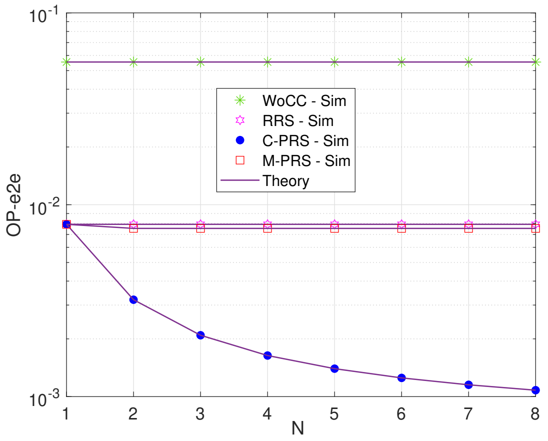

Fig. 3: OP-e2e as a function of N when $\Delta = 20$ (dB), $K = 5$, $\mathrm{R_{th}} = 0.25$ and $\alpha = 0.25$.

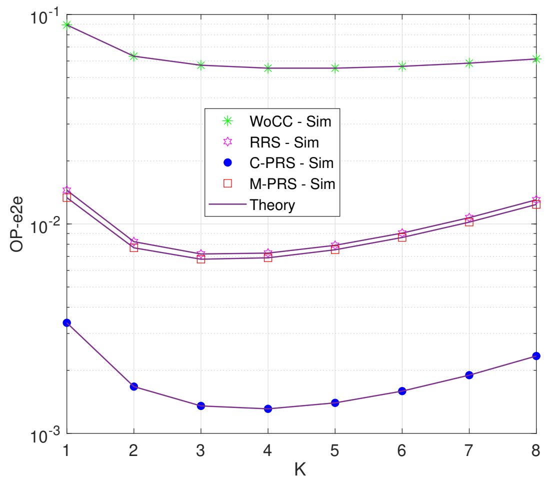

Fig. 4: OP-e2e as a function of $K$when $\Delta = 20$ (dB), $N = 5$, $\mathrm{R_{th}} = 0.25$ and $\alpha = 0.25$.

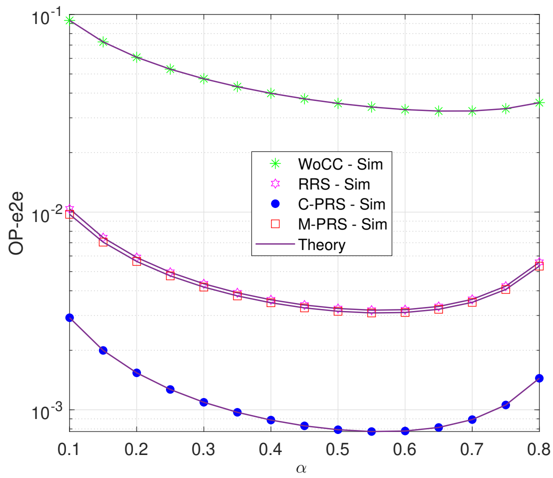

Fig. 5: OP-e2e as a function of α when $\Delta = 15$ (dB), $N = 3$, $\mathrm{R_{th}} = 0.1$ and $K = 4$.

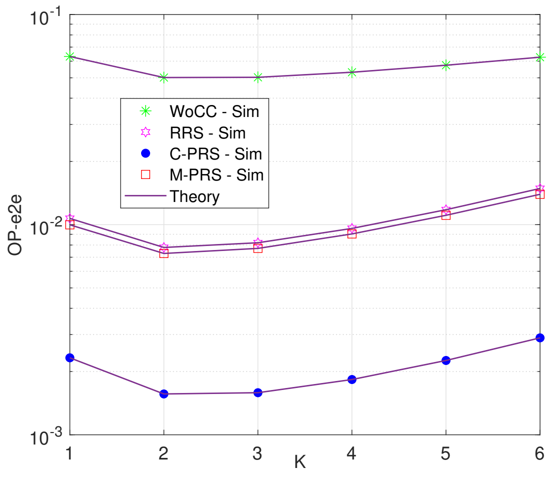

Fig. 6: OP-e2e as a function of K when $\Delta = 20$ (dB), $N = 5$ and $\mathrm{R_{th}} = 0.3$.

the best performance, which can be further enhanced by increasing the number of relays (N).

Fig. 4 investigates impact the number of hops (K)on the performance of the considered schemes when $\Delta = 20$ (dB), $N = 5$, $\mathrm{R_{th}} = 0.25$ and $\alpha = 0.25$. Fig. 4 presents that OP-e2e of all the schemes changes as increasing K from 1 to 8. It is worth noting that because $d_{\mathrm{M}_k\mathrm{M}_{k+1}} = 2d_{\mathrm{M}_k\mathrm{U}_k} = 2d_{\mathrm{U}_k M_{k+1}} = 1/K$, $\forall k$, hence, when K increases, the distances $d_{\mathrm{M}_k\mathrm{M}_{k+1}}$, $d_{\mathrm{M}_k\mathrm{U}_k}$ and $d_{\mathrm{U}_k M_{k+1}}$ decrease, and this is the reason why OP-e2e of all the schemes decreases. However, when K is high, the time allocated for each hop is small, and this reduces channel capacity obtained at each hop. As a result, we can observe from Fig. 4 that OP-e2e of all the schemes increases as K is high. Moreover, there exist optimal values of K at which OP-e2e of the considered schemes is lowest. In particular, the optimal number of hops of the C-PRS, M-PRS, RRS and WoCC schemes in Fig. 4 are 4, 3, 3 and 4, respectively.

Fig. 5 presents impact the fraction of the EH phases (α) on OP-e2e of all the considered schemes when $\Delta = 15$ (dB), $N = 3$, $\mathrm{R_{th}} = 0.1$ and $K = 4$. It is worth noting that if α is allocated with a high value, the transmit power of the transmitters is high, but the channel capacity obtained at each hop is low. As a result, as seen in Fig. 5, there exist optimal values of α (denoted by α^*_{Z}, where $\mathrm{Z} \in \{\text{C-PRS,M-PRS, RRS, WoCC}\}$. In particular, from Fig. 5, we have $\alpha^*_{\text{C-PRS}} = \alpha^*_{\text{M-PRS}} = \alpha^*_{\text{RRS}} = 0.55$ and $\alpha^*_{\text{WoCC}} = 0.65$. However, to find the exact value of α^*_{Z}, we can use one-dimensional search algorithm (or Golden Search algorithm) given in [24], and we have $\alpha^*_{\text{C-PRS}} = \alpha^*_{\text{M-PRS}} = \alpha^*_{\text{RRS}} = 0.565$ and $\alpha^*_{\text{WoCC}} = 0.6736$. Fig. 6 presents OP-e2e of the C-PRS, M-PRS, RRS and WoCC schemes as a func-

Tab. 1: Optimal value of α used for Fig. 6.

α^*_{Z}	$K=1$	$K=2$	$K=3$	$K=4$	$K=5$	$K=6$
WoCC	0.712	0.612	0.544	0.491	0.449	0.414
RRS	0.612	0.491	0.414	0.314	0.314	0.279
C-PRS	0.612	0.491	0.414	0.314	0.314	0.279
M-PRS	0.612	0.491	0.414	0.314	0.314	0.279

tion of K when $\Delta = 20$ (dB), $N = 5$ and $\mathrm{R_{th}} = 0.3$. In this figure, we use Golden Search algorithm [24] to find the values of α^*_{Z}, which are given in Table. 1. From Table. 1, we can see that the C-PRS, M-PRS, RRSschemes have the same value of α^*_{Y}. Furthermore, α^*_{Y} decreases with the increasing of K for all Y, and $\alpha^*_{\mathrm{WoCC}} > \alpha^*_{\mathrm{Y}}$, where $\mathrm{Y} \in \{\text{C-PRS}, \text{M-PRS}, \mathrm{RRS}\}$. We can observe from Fig. 6 that all the considered protocols achieve the best performance when $K = 2$.

5. Conclusion

This paper evaluated the OP-e2e performance of the C-PRS and M-PRS schemes via Monte-Carlo simulation and analysis. The obtained results indicate that our schemes achieve better performance, as compared with the corresponding RRS and WoCC ones. Moreover, the C-PRS scheme outperforms the M-PRS scheme in terms of outage probability and complexity implementation. Therefore, the C-PRS scheme should be selected for practical implementation. To further enhance the performance for the C-PRS and M-PRS schemes, important system parameters such as K, α and N should be optimally designed.

In future, full relay selection methods will be applied at each hop to enhance the OP-e2e performance for the multi-hop relaying schemes.

Author Contributions

The main contributions of Ngo Hoang An and Nguyen Trong Huan were to create the main ideas and execute performance evaluation by extensive simulations, while Ngoc-Lan Nguyen and Nguyen Tien Tung worked as the advisers of Ngo Hoang An and Nguyen Trong Huan to discuss, create, and advise the main ideas and performance evaluations together.

References

[1] TAN, N. N., et al. On the Dilemma of Reliability or Security in Unmanned Aerial Vehicle Communications Assisted by Energy Harvesting Relaying. *IEEE Journal on Selected Areas in Communications*. 2024, vol. 42, iss. 01, pp. 52-67. ISSN 0733-8716. DOI: 10.1109/JSAC.2023.3322756

[2] TAN, N. N., et al. Security-Reliability Trade-offs for Satellite–Terrestrial Relay Networks With a Friendly Jammer and Imperfect CSI. *IEEE Transactions on Aerospace and Electronic Systems*. 2023, vol. 59, iss. 05, pp. 7004-7019. ISSN: 0018-9251. DOI: 10.1109/TAES.2023.3282934

[3] TAN, N. N., et al. Physical Layer Security in AF-Based Cooperative SWIPT Sensor Networks. *IEEE Sensors Journal*. 2023, vol. 23, iss. 1, pp. 689-705. ISSN 1530-437X. DOI: 10.1109/JSEN.2022.3224128

[4] TAN, N. N., et al. Partial and Full Relay Selection Algorithms for AF Multi-Relay Full-Duplex Networks With Self-Energy Recycling in Non-Identically Distributed Fading Channels. *IEEE Transactions on Vehicular Technology*. 2022, vol. 71, iss. 6, pp. 6173-6188. ISSN 0018-9545. DOI: 10.1109/TVT.2022.3158340

[5] TAN, N. N., et al. Performance Enhancement for Energy Harvesting Based Two-Way Relay Protocols in Wireless Ad-hoc Networks with Partial and Full Relay Selection Methods. *Ad-hoc Networks*. 2019, vol. 54, pp. 178-187. ISSN 1570-8705. DOI: 10.1016/j.adhoc.2018.10.005

[6] TIN, P. T., et al. Throughput Enhancement for Multi-hop Decode-and-Forward Protocol using Interference Cancellation with Hardware Imperfection. *Alexandria Engineering Journal*. 2022, vol. 61, iss. 8, pp. 5837-5849. ISSN 2090-2670. DOI: 10.1016/j.aej.2021.11.008

[7] LE, A. T., et al. Performance Analysis of RIS-Assisted Ambient Backscatter Communication Systems. *IEEE Wireless Communications Letters*. 2024, vol. 13, iss. 3, pp. 791-795. ISSN 2162-2337. DOI: 10.1109/LWC.2023.3344113

[8] LUAN, N. T., LONG, N. T., VINH, N. V. and TIN, P. T. Outage Performance of Full-Duplex Unmanned Aerial Vehicle-aided Cooperative Non-orthogonal Multiple Access. *Advances in Electrical and Electronic Engineering*. 2023, vol. 21, iss. 03, pp. 1-8. ISSN 1336-1376. DOI: 10.15598/aeee.v21i1.4515

[9] SANG, N. Q., TAN, N. N. and TU, L. T. On the security and reliability performance of SWIPT-enabled full-duplex relaying in the non-orthogonal multiple access networks. *Journal of Information and Telecommunication*. 2023, vol. 7, iss. 04, pp. 462-476. ISSN 2475-1839. DOI: 10.1080/24751839.2023.2218046

[10] TAN, N. N., et al. On the performance of underlay device-to-device communications. *Sensors*. 2022, vol. 22, iss. 04, ID 1456. ISSN 1424-8220. DOI: 10.3390/s22041456

[11] NAM, P. M., et al. Outage performance of interference cancellation-aided two-way relaying cognitive network with primary TAS/SC communication and secondary partial relay selection. *Electronics*. 2022, vol. 11, iss. 22, ID 3645. ISSN 2079-9292. DOI: 10.3390/electronics11223645

[12] DUY, T. T., ALEXANDROPOULOS, G. C., VU, T. T., SON, V. N. and DUONG, T. Q. Outage Performance of Cognitive Cooperative Networks with Relay Selection over Double-Rayleigh Fading Channels. *IET Communications*. 2016, vol. 10, iss. 01, pp. 57-64. ISSN 1751-8628. DOI: 10.1049/iet-com.2015.0236

[13] SANG, N. Q., et al. Secrecy Outage Performance Analysis of Vehicular DF Relaying Network under Underlay Cognitive Power Constraint and Physical-Layer Security. In: *The 7th International Conference on Advanced Engineering – Theory and Applications (AETA 2022)*. HoChiMinh city, Vietnam, 2022, pp. 1–12. ISBN 978-981-99-8702-3. DOI: 10.1007/978-981-99-8703-0_58

[14] CHIEN, T. V., TU, T. L., CHATZINOTAS, S. and OTTERSTEN, B. Coverage Probability and Ergodic Capacity of Intelligent Reflecting Surface-Enhanced Communication Systems. *IEEE Communications Letters*. 2021, vol. 25, iss. 01, pp. 69-73. ISSN 1089-7798. DOI: 10.1109/LCOMM.2020.3023759

[15] CHIEN, T. V., et al. Outage Probability Analysis of IRS-Assisted Systems Under Spatially Correlated Channels. *IEEE Wireless Communications Letters*. 2021, vol. 10, iss. 8, pp. 1815-1819. ISSN 2162-2345. DOI: 10.1109/LWC.2021.3082409

[16] TIN, P. T., HUNG, D. T., DUY, T. T. and VOZNAK, M. Security-Reliability Analysis of NOMA – Based Multi-Hop Relay Networks In Presence Of an Active Eavesdropper With Imperfect Eavesdropping CSI. *Advances in Electrical and Electronic Engineering*. 2017, vol. 15, iss. 04, pp. 591-597. ISSN 1336-1376. DOI: 10.15598/aeee.v15i4.2386

[17] VAN, N. T., DINH, N. V., COSTA, D. B. da, AN, B. Short-Packet Communications in Multi-Hop WPINs: Performance Analysis and Deep Learning Design. In: *2021 IEEE Global Communications Conference (GLOBECOM)*. Madrid, Spain, 2021, pp. 1–6. ISBN 978-1-7281-8104-2. DOI:: 10.1109/GLOBECOM46510.2021.9685765

[18] TU, T. L., et al. Performance Analysis of Multi-hop Full-duplex NOMA Systems With Imperfect Interference Cancellation and Near-Field Path-Loss. *Sensors*. 2023, vol. 23, iss. 01, ID 524. ISSN 1424-8220. DOI: 10.3390/s23010524

[19] NAM, P. M., CA, P. V., TUAN, P. V., DUY, T. T. and BAO, V. N. Q. Security versus Reliability Study for Multi-hop Cognitive M2M Networks With Joint Impact of Interference Constraint and Hardware Noises. In: *2018 International Conference on Advanced Technologies for Communications (ATC)*. HoChiMinh city, Vietnam, 2018, pp. 259-264. DOI: 10.1109/ATC.2018.8587460

[20] TY, V. T., et al. Security-Reliability Trade-off of Multi-hop Secure Communication Networks Using Fountain Codes and RIS-aided Cooperative Communication. In: *2023 International Conference on Advanced Technologies for Communications (ATC)*. Da Nang, Vietnam, 2023, pp. 499-504. ISBN 979-8-3503-0132-8. DOI: 10.1109/ATC58710.2023.10318517

[21] XU, C., ZHENG, M., LIANG, W., YU, H. and LIANG, Y. C. Outage Performance of Underlay Multihop Cognitive Relay Networks With Energy Harvesting. *IEEE Communications Letters*. 2016, vol. 20, iss. 6, pp. 1148-1151. ISSN 1089-7798. DOI: 10.1109/LCOMM.2016.2547985

[22] XU, C., ZHENG, M., LIANG, W., YU, H. and LIANG, Y. C. End-to-End Throughput Maximization for Underlay Multi-Hop Cognitive Radio Networks With RF Energy Harvesting. *IEEE Transactions on Wireless Communications*. 2017, vol. 16, iss. 06, pp. 3561-3572. ISSN 1536-1276. DOI: 10.1109/TWC.2017.2684125

[23] HIEU, T. D., DUY T. T. and KIM, B. S. Performance Enhancement for Multi-hop Harvest-to-Transmit WSNs With Path-Selection Methods in Presence of Eavesdroppers and Hardware Noises. *IEEE Sensors Journal*. 2018, vol. 18, iss. 12, pp. 5173 – 5186. ISSN 1530-437X. DOI: 10.1109/JSEN.2018.2829145

[24] NAM, P. M., DUY, T. T., CA, P. V., SON, P. N. and AN, N. H. Outage Performance of Power Beacon-Aided Multi-Hop Cooperative Cognitive Radio Protocol Under Constraint of Interference and Hardware Noises. *Electronics*. 2020, vol. 9, iss. 6, ID 1054. ISSN 2079-9292. DOI: 10.3390/electronics9061054

[25] VAN, N. T., et al. Short-Packet Communications in Multi Hop Networks with WET: Performance Analysis and Deep Learning-Aided Optimization. *IEEE Transactions on Wireless Communications*.

2023, vol. 22, iss. 01, pp. 439-456. ISSN 1536-1276. DOI: 10.1109/TWC.2022.3195234

[26] HUAN, N. T., et al. Incremental Cooperation Based Multi-hop Relaying Scheme With Fountain Codes, Wirelessly Energy Harvesting and Partial Relay Selection. In: *2022 International Conference on Advanced Technologies for Communications (ATC)*. HaNoi, Vietnam, 2022, pp. 338-343. ISBN 978-1-6654-5188-8. DOI: 10.1109/ATC55345.2022.9943044

[27] SANG, N. Q. and KONG, H. Y. Generalized diversity combining of energy harvesting multiple antenna relay networks: outage and throughput performance analysis. *Annals of Telecommunications*. 2016, vol. 71, pp. 265-277. ISSN 0003-4347. DOI: 10.1007/s12243-016-0508-9

[28] TU, T. L. and TIEP, H. M. Cooperative spectrum-sharing with two-way AF relaying in the presence of direct communications. *EAI Endorsed Transactions on Industrial Networks and Intelligent Systems*. 2018, vol. 5, iss. 14, pp. 1-9. ISSN: 2410-0218. DOI: 10.4108/eai.27-6-2018.154836

[29] SANG, N. Q. and KONG, H. Y. Outage probability analysis in dual-hop vehicular networks with the assistance of multiple access points and vehicle nodes. *Wireless Personal Communications*. 2016, vol. 87, pp. 1175-1190. ISSN 0929-6212. DOI: 10.1007/s11277-015-3047-1

[30] MINH, P. X., et al. Performance of Energy Harvesting Aided Multi-hop Mobile Relay Networks With and Without Using Cooperative Communication. In: *2023 International Conference on System Science and Engineering (ICSSE)*. HoChiMinh city, Vietnam, 2023, pp. 620-625. ISBN 979-8-3503-2294-1. DOI: 10.1109/ICSSE58758.2023.10227223

[31] VO, D. T., et al. SWIPT-Enabled Cooperative Wireless IoT Networks With Friendly Jammer and Eavesdropper: Outage and Intercept Probability Analysis. *IEEE Access*. 2023, vol. 11, pp. 86165-86177. ISSN 2169-3536. DOI: 10.1109/ACCESS.2023.3303369

[32] GRADSHTEYN, I. S. and RYZHIK I. M. Table of Integrals, Series, and Products. *Boston: Academic Press*, 2007. ISBN 978-0-12-384933-5